



Published in final edited form as:

*Mol Cell Biochem.* 2011 September ; 355(1-2): 135–148. doi:10.1007/s11010-011-0847-9.

## ACYL-CoA BINDING PROTEINS INTERACT WITH THE ACYL-CoA BINDING DOMAIN OF MITOCHONDRIAL CARNITINE PALMITOYL TRANSFERASE I

Heather A. Hostetler<sup>a,b</sup>, Dan Lupas<sup>c</sup>, Yingran Tan<sup>c</sup>, Jia Dai<sup>c</sup>, Matthew S. Kelzer<sup>b</sup>, Gregory G. Martin<sup>a</sup>, Gebre Woldegiorgis<sup>c</sup>, Ann B. Kier<sup>d</sup>, and Friedhelm Schroeder<sup>a,\*</sup>

<sup>a</sup>Department of Physiology and Pharmacology, Texas A&M University, TVMC, College Station, TX 77843

<sup>b</sup>Department of Biochemistry & Molecular Biology, Boonshoft School of Medicine, Wright State University, Dayton, OH 45435

<sup>c</sup>Department of Environmental and Biomolecular Systems, OGI School of Science and Engineering, Oregon Health and Science University, Beaverton, OR 97006

<sup>d</sup>Department of Pathobiology, Texas A&M University, TVMC, College Station, TX 77843

### Abstract

Although the rate limiting step in mitochondrial fatty acid oxidation, catalyzed by carnitine palmitoyltransferase I (CPTI), utilizes long-chain fatty acyl-CoAs (LCFA-CoA) as a substrate, how LCFA-CoA are transferred to CPTI remains elusive. Based on secondary structural predictions and conserved tryptophan residues, the cytoplasmic C-terminal domain was hypothesized to be the LCFA-CoA binding site and important for interaction with cytoplasmic LCFA-CoA binding/transport proteins to provide a potential route for LCFA-CoA transfer. To begin to address this question, the cytoplasmic C-terminal region of liver CPTI (L-CPTI) was recombinantly expressed and purified. Data herein show for the first time that the L-CPTI C-terminal 89 residues were sufficient for high affinity binding of LCFA-CoA ( $K_d = 2\text{--}10\text{nM}$ ) and direct interaction with several cytoplasmic LCFA-CoA binding proteins ( $K_d < 10\text{nM}$ ), leading to enhanced CPTI activity. Furthermore, alanine substitutions for tryptophan in L-CPTI (W391A and W452A) altered secondary structure, decreased binding affinity for LCFA-CoA, and almost completely abolished L-CPTI activity, suggesting that these amino acids may be important for ligand stabilization necessary for L-CPTI activity. Moreover, while decreased activity of the W452A mutant could be explained by decreased binding of lipid binding proteins, W391 itself seems to be important for activity. These data suggest that both interactions with lipid binding proteins and the peptide itself are important for optimal enzyme activity.

### Keywords

Carnitine palmitoyltransferase I; L-CPTI; long-chain fatty acyl-CoA; Acyl-CoA Binding Site; FRET Analysis

---

\*To whom correspondence should be addressed: Department of Physiology and Pharmacology, Texas A&M University, TVMC, College Station, TX 77843-4466. Phone: (979) 862-1433, FAX: (979) 862-4929, fschroeder@cvm.tamu.edu.

## INTRODUCTION

Liver is the major organ for taking up and metabolizing dietary long chain fatty acids (LCFAs). Hepatocytes quickly convert LCFAs to their activated CoA thioesters (LCFA-CoAs) for rapid delivery to oxidative organelles, such as mitochondria, in order to produce much of the energy needed for multiple hepatocyte functions [1]. Spontaneous LCFA-CoA transfer to mitochondria is unlikely to account for this rapid delivery, since LCFA-CoAs are poorly water soluble, readily degrade in aqueous systems, and are highly membrane-bound [2, 3]. Furthermore, the rate limiting step in mitochondrial LCFA oxidation is the conversion of LCFA-CoA to LCFA-carnitine mediated by carnitine palmitoyl transferase-I (CPTI) in the mitochondrial outer membrane [4]. *In vitro* studies show that CPTI itself is inhibited by high levels of substrate LCFA-CoAs [4, 5]. While BSA as a vehicle prevents LCFA-CoA substrate inhibition to enhance CPTI activity for *in vitro* assays, BSA is a secreted protein not normally present in cytoplasm [4, 5]. Although indirect evidence has suggested that CPTI might need to recognize both the LCFA-CoA and a LCFA-CoA binding protein to acquire the LCFA-CoA [6], it is unclear whether intracellular LCFA-CoA binding proteins directly interact with CPTI to enhance CPTI activity. Due to CPTI's central role in LCFA oxidation, a thorough understanding of the molecular mechanism of regulation of CPT is an important first step in the development of treatments for diseases such as myocardial ischemia, heart failure, diabetes, obesity, cancer, and inherited CPT deficiency diseases [7–9].

Liver expresses at least three different families of cytoplasmic LCFA-CoA binding proteins: acyl-CoA binding protein (ACBP) (review in [10, 11]; liver fatty acid binding protein (L-FABP) (review in [12, 13], sterol carrier protein-2 (SCP-2) (review in [14, 15]. Studies *in vitro* and in transfected cells overexpressing the respective cytoplasmic LCFA-CoA binding proteins show that they enhance LCFA-CoA desorption from membranes, increase aqueous solubility and stability of LCFA-CoAs, enhance intracellular transfer of bound ligands, and stimulate LCFA-CoA transacylation to form glycerides and cholesteryl esters (review in [10, 12, 15]. Tissue levels of the cytoplasmic LCFA-CoA binding proteins correlate with LCFA oxidative ability [16, 17]. Further, overexpression of L-FABP or SCP-2 enhances LCFA oxidation while ablation of L-FABP or SCP-2 diminishes LCFA oxidation [18–21]. However, it is not known whether any of the cytoplasmic LCFA-CoA binding proteins enhance CPTI simply by increasing LCFA-CoA solubility to prevent LCFA-CoA substrate inhibition or if the cytoplasmic LCFA-CoA binding proteins directly interact with CPTI to enhance mitochondrial LCFA oxidation.

Although direct evidence demonstrating that the cytoplasmic facing 89 amino acids of the liver CPTI (L-CPTI) C-terminus represents the ligand binding domain and/or may interact with LCFA-CoA binding proteins is lacking, this possibility is suggested by reduced CPTI activity found when amino acids in this region are mutated, as well as sequence homology with other LCFA-CoA binding proteins [5, 22–25]. The finding that tryptophan residues 391 and 452 in L-CPTI are highly conserved further suggested that these specific residues may be important for LCFA-CoA binding and/or transfer from cytoplasmic LCFA-CoA binding proteins. Since purified full-length CPT-I protein was found to be completely inactivated when removed from its natural environment (membranes), and since membranes themselves will uptake LCFA-CoA [6], the studies described herein utilized the C-terminal 89 amino acid domain of L-CPTI WT to determine if this region: (i) binds specific cytoplasmic LCFA-CoA binding proteins; (ii) tryptophans at residues 391 and 452 are important for interaction with cytoplasmic LCFA-CoA binding proteins; (iii) exhibits high affinity for LCFA-CoA; (iv) tryptophans at residues 391 and 452 are important for high affinity LCFA-CoA binding.

## EXPERIMENTAL PROCEDURES

### Construction of plasmids for expression of wild-type and mutant 89-residue L-CPTI peptides

The C-terminal region (residues 381–469) of the rat wild-type L-CPTI (WT) and tryptophan mutants (W391A and W452A) were PCR amplified using the primers P89 forward, 5'-GGAATTCCATATGGCCGCCCTCACTGCTGCA-3' and P89 reverse, 5'-GGCCGCTCGAGCTATTATATGCCTATCTTGCTGTT-3' with NdeI and XhoI restriction sites [22]. To construct the N-terminally His-tagged peptides, the 267-bp PCR products were subcloned into the NdeI-XhoI linearized bacterial expression vector pPROEX-1 (Invitrogen, Carlsbad, CA), and the mutations were confirmed by DNA sequencing.

### Expression of wild-type and mutant 89-residue L-CPTI peptides in *E. coli*

pPROEX-wild type and mutant plasmids were transformed into BL21(DE3) *E. coli* cells, and an overnight culture of each was used to inoculate 10L of LB medium containing 100µg/ml ampicillin. Cultures were grown at 37°C with constant shaking to an  $A_{600}$  of 0.5–0.8, induced with 1.0mM IPTG, and incubated for an additional 5h. Cells were harvested by centrifugation, washed with 100ml of lysis buffer (15mM Tris, pH 8.0, 300mM NaCl; 10mM imidazole; 1mM PMSF; 0.2% Protease Inhibitor; 1µg/ml Leupeptin) per liter culture, resuspended in 10ml of lysis buffer per liter culture, and then lysed by French press. Octylglucoside was added to the cell lysate to a final concentration of 1%, and the lysate was incubated for 30 min at 4°C. The insoluble cell debris was removed by centrifugation, and the peptides were purified from the clear supernatant (lysate) as described below.

### Purification of wild-type and mutant 89-residue L-CPTI peptides

Ni-NTA resin (1 mL per 2 mL of cell lysate; Qiagen Inc., Valencia, CA) was equilibrated with lysis buffer containing 1% octylglucoside and 20 mM imidazole, mixed with cell lysate, and incubated at 4°C overnight in the column. Lysate was allowed to flow through the column by gravity. The column was washed 5-times with the lysis buffer containing 20 mM imidazole and 1% octylglucoside. The His-tagged 89-residue L-CPTI fragments were then eluted with lysis buffer containing 250 mM imidazole in 4.0 mL fractions. Fractions were examined by SDS-PAGE using 16.5% Tris-Tricine gels under reducing conditions and either stained with Coomassie blue or transferred to nitrocellulose membranes and incubated with anti-His tag antibodies (Qiagen, Valencia, CA) as described previously [5]. Fractions containing His-tagged peptides were pooled, concentrated with Centricon Plus-Y3 Centrifugal Filter Devices with Ultracel PL Membranes, and desalted such that the final NaCl and imidazole concentrations were 15 mM and <0.2 mM, respectively. These samples were further purified by gel filtration chromatography on Sephadex G-50 columns (Sigma, St. Louis, MO) and eluted in 10 mM Tris-HCl buffer. Purity and identity of the fractions were confirmed by SDS-PAGE, Coomassie blue staining, and Western blotting. Fractions containing L-CPTI peptides as a single band at the expected molecular weight were further concentrated by centrifugation (centriplus YM-3). Each protein was resuspended in a protease inhibitor cocktail mixture with 1% octylglucoside prior to and following each purification step. Protein concentrations were determined using the Bio-Rad protein assay kit.

### Expression and purification of recombinant lipid binding proteins

Mouse recombinant ACBP protein was expressed and purified as previously described [26]. Mouse recombinant L-FABP protein was produced, purified, and delipidated as previously described [27]. Human recombinant SCP-2 was produced as described earlier [14]. Cytochrome C was purchased from Sigma Aldrich (St. Louis, MO).

### Secondary structure determination: circular dichroism

Circular dichroism was used to determine whether interaction of the 89-residue wild-type or mutant peptides with lipid binding proteins resulted in protein conformational changes. Circular dichroic (CD) spectra of each of the CPTI (wild type, W391A, W452A) peptides (3.4 $\mu$ M), ACBP (3.3 $\mu$ M), L-FABP (2.4 $\mu$ M), SCP-2 (2.2 $\mu$ M), Cytochrome C (2.9 $\mu$ M), [1.7 $\mu$ M CPTI peptide + 1.65 $\mu$ M ACBP], [1.7 $\mu$ M CPTI peptide + 1.2 $\mu$ M L-FABP], [1.7 $\mu$ M CPTI peptide + 1.1 $\mu$ M SCP-2], and [1.7 $\mu$ M CPTI peptide + 1.45 $\mu$ M Cytochrome C] (final amino acid molarity in each sample was equal to 0.0003M) in 50 $\mu$ M tris, pH 7.2 and 0.0005% octylglucoside were obtained with a J-810 spectropolarimeter (JASCO Inc., Easton, MD) at 23°C in a 1-mm cuvette as previously described [28, 29]. Replicate spectra were recorded from 260 to 185nm with a bandwidth of 2nm, sensitivity of 10 millidegrees, scan rate of 50nm/min, and a time constant of 1s. The percentage of secondary structures ( $\alpha$ -helices,  $\beta$ -strands, turns, and unordered structures) was determined with the software package CDPro (downloaded from the website: <http://lamar.colostate.edu/~sreeram/CDPro>) [30]. The CD spectrum of the mixed proteins was compared to a theoretical spectrum of combined but non-interacting proteins, which was calculated by averaging the spectra of each protein analyzed separately at a concentration equal to that in the mixture [29].

### Fluorescence resonance energy transfer between CPTI peptides and lipid binding proteins

The 89-residue wild type and mutant L-CPTI peptides were fluorescently labeled with Cy3 dye, while recombinant ACBP, L-FABP, SCP-2, and Cytochrome C proteins were fluorescently labeled with Cy5 dyes, using the Fluorolink-antibody Cy3 and Cy5 labeling kits (Amersham Biosciences, Pittsburgh, PA). Absorbance and mass spectroscopy measurements [31] were used to determine protein concentrations, as well as dye to protein ratios, and labeling ratios were maintained at approximately 1 dye per peptide or protein molecule. Emission spectra (560–700nm) were obtained of 30nM donor (Cy3-labeled CPTI peptides) in PBS at 24°C upon excitation at 550nm with increasing concentration of acceptor (Cy5-labeled ACBP, L-FABP, SCP-2, or Cytochrome C) in a PC1 photon counting spectrofluorometer (ISS Inc., Champaign, IL) as previously described for other proteins with this donor/acceptor pair [29, 31]. The spectra were corrected for background (buffer only and acceptor only) and the maximal intensities measured using Vinci 1.5 software (ISS Inc., Champaign, IL). The protein binding affinity and the energy transfer efficiency were calculated using the amount of sensitized acceptor fluorescence, and the intermolecular distance was calculated according to the Förster equation as described earlier [28, 29, 31].

### CPTI assay

Carnitine palmitoyl transferase I activity was determined in isolated mitochondria from the yeast strains expressing the wild-type and mutant CPTIs by the forward exchange method using L-[methyl-<sup>3</sup>H] carnitine as described previously [32, 33]. The activity was measured by varying the palmitoyl-CoA to BSA, ACBP, L-FABP, and SCP-2 molar ratios from 1.85 to 7.41 at a fixed carnitine concentration of 1.0 mM as described previously [32, 33]. Mitochondrial protein (150 $\mu$ g) was used, and all incubations were performed at 30°C for 5 min. Reactions were stopped by addition of 6% perchloric acid and processed as described [32, 33].

### Direct binding of naturally-occurring fluorescent LCFA-CoA (cis-parinaroyl-CoA)

Direct ligand binding assays not requiring separation of protein-bound from free ligand were performed using *cis*-parinaroyl-CoA, a naturally-occurring fluorescent LCFA-CoA which has a structure similar to endogenous LCFA-CoA [28]. Fluorescent *cis*-parinaroyl-CoA was synthesized from *cis*-parinaric acid (Cayman Chemicals, Ann Arbor, MI) and purified by HPLC as previously described [34]. Increasing concentrations of fluorescent ligand (0–500

nM) were added from a concentrated stock to 0.1  $\mu$ M of purified wild-type or mutant peptide in 2 ml of phosphate-buffered saline (pH 7.4). Fluorescence emission spectra were obtained at 24°C with an SLM 8000C spectrofluorometer (SLM Aminco Instruments, Rochester, NY) upon excitation of *cis*-parinaroyl-CoA at 310nm, corrected for background (protein only and fluorescent ligand only), and maximal intensities measured. The dissociation constant and the number of binding sites were obtained by a double reciprocal plot of the fluorescence intensity at a given concentration of ligand as described previously [35]. The saturation curves were fitted to a Hill plot to confirm the number of binding sites obtained [28].

#### **Displacement of bound fluorescent *cis*-parinaroyl-CoA by endogenous non-fluorescent LCFA-CoA (palmitoyl-CoA)**

In order to determine whether the ligand binding seen with *cis*-parinaroyl-CoA also occurred with endogenous, non-fluorescent ligands, the ability of palmitoyl-CoA to displace the bound fluorescent ligand (*cis*-parinaroyl-CoA) was examined as described previously [28]. The 89-residue L-CPTI peptide (0.1  $\mu$ M in phosphate-buffered saline, pH 7.4) was incubated with *cis*-parinaroyl-CoA (50 nM) for 5 min at 24°C to obtain maximal fluorescence. Excitation of *cis*-parinaroyl-CoA occurred at 310 nm, and emission was measured at 426 nm with an SLM 8000C spectrofluorometer (SLM Aminco Instruments, Rochester, NY). The displacement of bound fluorescent ligand was calculated from the decrease in *cis*-parinaroyl-CoA fluorescence intensity with increasing concentrations of palmitoyl-CoA. The  $K_i$  values for each peptide were then calculated as described previously [35].

#### **Quenching of intrinsic fluorescence of the 89-residue wild-type and mutant peptides by endogenous non-fluorescent LCFA-CoA (palmitoyl-CoA)**

The wild type 89-residue peptide contains two tryptophans with intrinsic steady state fluorescence separated by 60 amino acid residues. Binding of the nonfluorescent ligand, such as palmitoyl-CoA, is expected to quench the intrinsic steady state fluorescence of the WT 89 residue peptide, but not of the Trp mutants. To estimate palmitoyl-CoA binding to the peptide residues, direct binding of the nonfluorescent ligands to the 89 residue peptides was determined as described previously [28, 35]. Briefly, the 89 residue peptides (0.1  $\mu$ M in 2 ml of phosphate-buffered saline, pH 7.4) were titrated with increasing levels of palmitoyl-CoA (0–150 nM). The intrinsic fluorescence of the aromatic amino acids within the peptides was excited at 280 nm, and fluorescence emission was measured from 300 to 450 nm. The dissociation constant and number of binding sites were calculated by a double reciprocal plot as previously described [28, 35]. The saturation curves were fitted to a Hill plot to confirm the number of binding sites obtained above.

#### **Fluorescence resonance energy transfer and determination of intermolecular distance between CPTI and *cis*-parinaroyl-CoA**

Fluorescence resonance energy transfer (FRET) from the aromatic amino acids within the 89-residue L-CPTI wild-type and mutant peptides to *cis*-parinaroyl-CoA was conducted as previously described for PPAR $\alpha$  and *cis*-parinaroyl-CoA [28]. The 89-residue CPTI peptides (0.1 $\mu$ M in 2mls of PBS, pH 7.4) were titrated with increasing amounts of *cis*-parinaroyl-CoA (0–1000nM), and CPTI aromatic amino acid excitation was carried out at 280nm with emission scan from 300–450nm on an ISS PC1 photon counting spectrofluorometer (ISS Inc., Champaign, IL) at 24°C. The intermolecular distance between CPTI and bound ligand was calculated according to the Förster equation as described earlier [28].

## Statistics

Values represented the mean  $\pm$  SE with n and P indicated as described. Statistical analyses were performed using Student's *t*-test or two-way analysis of variance (ANOVA) (GraphPad Prism, San Diego, CA). Values with  $P < 0.05$  were considered statistically significant.

## RESULTS

### Effect of C-terminal mutations on secondary structure of L-CPTI: circular dichroism

The importance of the C-terminal amino acid residues 391 and 452 to secondary structure of L-CPTI was determined by CD. While the alanine substitution at position 391 resulted in increased ellipticity at 193nm and more negative ellipticity at 222nm, the alanine substitution at position 452 had an opposite effect (Fig. 1). These strong structural changes corresponded to increased  $\alpha$ -helical and decreased  $\beta$ -sheet content for the W391A mutant, while the W452A mutant was comprised of very little  $\alpha$ -helices and showed an increase in  $\beta$ -sheets (Table 1). Thus, although the W391A and W452A mutant peptides remained highly ordered, the respective alanine substitutions significantly altered L-CPTI secondary structure —albeit in opposite directions. How these diametrically opposite secondary structural changes affected L-CPTI function was addressed in the following sections.

### CPTI peptides directly interacted with lipid binding proteins: circular dichroism

Potential interactions of WT L-CPTI peptides with cytoplasmic LCFA-CoA binding/transfer proteins (ACBP, L-FABP, SCP-2) were examined by CD. Interactions of WT L-CPTI peptides with cytochrome C (CytoC) were examined as a control. The experimentally obtained (actual, *filled circles*) CD spectra of WT CPTI with ACBP (Fig. 2a), L-FABP (Fig. 2b), SCP-2 (Fig. 2c), and CytoC (Fig. 2d) were compared to the theoretical spectrum of each that would be obtained if no protein interaction occurred (theoretical, *open circles*). Significant differences were noted in the WT CPTI spectra with each of the lipid binding proteins, while no significant differences were noted with CytoC, indicating that the C-terminal region of CPTI directly interacted with ACBP, L-FABP, and SCP-2. Quantitative analysis of multiple replicates for percent composition of secondary structures confirmed these conclusions (Table 2).

### Fluorescence resonance energy transfer between Cy3- and Cy5- labeled L-CPTI WT peptide and cytoplasmic LCFA-CoA binding proteins: binding affinity and intermolecular distance

To further establish the direct binding and intermolecular distance between WT L-CPTI and cytoplasmic LCFA-CoA binding proteins, the respective recombinant peptides/proteins were fluorescently labeled with small fluorescent tags (Cy3 or Cy5, respectively). The Cy3/Cy5 tags form an efficient donor/acceptor pair for FRET, which is useful for examining protein-protein interactions [29, 31, 36]. This FRET assay allowed for determination of: (i) the WT CPTI affinity for each of the cytoplasmic LCFA-CoA binding proteins; (ii) the distance between CPTI and the lipid binding proteins; and (iii) the effect of the tryptophan mutations on these interactions.

The donor (Cy3-labeled WT CPTI) was excited at 550nm and fluorescence emission measured from 560 to 700nm to allow the fluorescence signal from Cy3 and Cy5 to be detected (Fig. 3a). Upon titration of Cy3-CPTI with Cy5-ACBP (data not shown), Cy5-L-FABP (Fig. 3a), or Cy5-SCP-2 (data not shown), the Cy3-CPTI fluorescence was quenched at approximately 570nm and sensitized emission of Cy5 was observed at 670nm, indicative of FRET. However, titration with Cy5-Cytochrome C resulted in only minor changes and no FRET or binding was observed (data not shown). By plotting the increase of Cy5 fluorescence as a function of Cy5-L-FABP concentration, a saturable ligand binding curve

was obtained (Fig. 3b), indicating high affinity binding. By plotting the data as a double reciprocal plot (Fig. 3b, inset), a linear line was obtained, consistent with a single binding site. Similar binding curves were obtained for Cy5-ACBP and Cy5-SCP-2, showing that the C-terminal region of WT L-CPTI binds all 3 lipid binding proteins with high affinity ( $K_d < 10\text{nM}$ , Table 3). These proteins all exhibited close molecular interaction with similar intermolecular distances (Table 3), supporting the results obtained by CD and suggesting that the C-terminal region of L-CPTI is sufficient for LCFA-CoA binding protein interactions.

### FRET between mutant CPTI peptides and lipid binding proteins

To examine the importance of the C-terminal tryptophans on the interaction between L-CPTI and cytoplasmic LCFA-CoA binding proteins, the above FRET experiments were repeated with the W391A and W452A peptides. FRET was observed as quenching of Cy3-W391A (Fig. 3c) and Cy3-W452A (Fig. 3e) fluorescence and increased Cy5 fluorescence upon titration with Cy5-L-FABP. Similar results were obtained with Cy5-ACBP and Cy5-SCP-2 (data not shown). The change in fluorescence intensity at 670nm again gave strong saturable binding by Cy5-L-FABP (Fig. 3d), and similar binding affinities ( $K_d < 10\text{nM}$ ) were obtained with the W391A peptide as the WT peptide (Table 3). Although the W391A peptide gave similar binding affinities as the WT peptide, some variation was noted in the intermolecular distances between the CPTI peptide and the cytoplasmic LCFA-CoA binding proteins, especially SCP-2 (Table 3). In contrast, mutation of the tryptophan at position 452 to alanine resulted in substantially reduced binding affinities (Fig. 3f) and increased intermolecular distances as compared to the WT peptide (Table 3). This “discrepancy” of W391A resulting in changes of intermolecular distance, but not binding affinity, suggested that the conformational changes noted in Fig. 1 altered the distance between the fluorophores but that such structural changes did not alter the region required for binding of lipid binding proteins. Since the W452A peptide showed both weaker affinities and greater distances, it is likely that both the structural changes (seen in Fig. 1) and the actual tryptophan at 452 are important for CPTI interaction with lipid binding proteins. Thus, these data suggested that even though both mutations resulted in conformational changes, the tryptophan residue at position 452 is more important for L-CPTI interaction with cytoplasmic LCFA-CoA binding proteins and may play an important role in protein-protein stabilization.

### L-CPTI activity

Since earlier findings suggested that the highly conserved C-terminal tryptophan residues may be involved in CPTI activity [22], this possibility was tested with the C-terminal 89-residue L-CPTI and mutant peptides. Due to substrate inhibition by LCFA-CoA, L-CPTI activity is negligible in the absence of LCFA-CoA carrier proteins and therefore BSA is typically used as a LCFA-CoA vehicle in CPTI activity assays [4, 5]. Although a small concentration of BSA in the CPT-1 activity assay resulted in robust activity, increasing BSA concentration was somewhat inhibitory—consistent with increasing competition of BSA with CPTI for LCFA-CoA ligand (Table 4). Highest CPTI activity was observed in the order WT L-CPTI  $\gg$  W391A  $\gg$  W452A at each BSA concentration examined (Table 4). These data establish that the highly conserved C-terminal tryptophan residues at positions 391 and 452 are essential for optimal L-CPTI activity.

Since BSA is a secreted/extracellular protein not normally found in the cytoplasm, the above assays were repeated using equimolar amounts of cytoplasmic LCFA-CoA binding proteins (ACBP, L-FABP, or SCP-2). At low LCFA-CoA binding protein concentrations (high ratio of palmitoyl-CoA to protein), the WT L-CPTI peptide exhibited high activity in the presence of ACBP or SCP-2 similar to that observed with BSA (Table 4). Addition of L-FABP

elicited slightly higher L-CPTI activity—especially at higher L-FABP concentrations—as compared to BSA (Table 4). However, the L-FABP advantage was abolished by the W391A mutation, and increasing L-FABP protein concentrations had no further effect on L-CPTI activity (Table 4). Mutation of Trp452 to Ala resulted in almost no L-CPTI (Table 4).

### **Effect of C-terminal mutations on L-CPTI binding of LCFA-CoA: direct fluorescent ligand binding assay**

Since the decreased activity for W452A, but not W391A, could be explained in part by decreased L-CPTI interactions with cytoplasmic LCFA-CoA binding proteins, the contribution of these conserved tryptophans in LCFA-CoA binding was also examined. *Cis*-parinaroyl-CoA, a non-metabolizable fluorescent LCFA-CoA of 18 carbons and 4 *cis*-double bonds, was utilized to demonstrate that the 89 residue C-terminal peptide was sufficient for LCFA-CoA binding and to determine the effect of the W391A and W452A mutations on this affinity. The fluorescence emission intensity of *cis*-parinaroyl-CoA (after background correction) was saturable upon titration of the WT peptide with increasing concentrations of *cis*-parinaroyl-CoA (Fig. 4a). A double reciprocal plot of these data resulted in a linear plot (Fig. 4a, inset), indicating a single high-affinity binding site with  $K_d = 9 \pm 1 \text{ nM}$ . Although both L-CPTI mutants also showed saturable binding at a single binding site (data not shown), these binding affinities were 5–7 fold weaker than obtained for the WT (Table 5). These data suggest that the C-terminal region of L-CPTI is responsible for LCFA-CoA binding and that the tryptophan residues at positions 391 and 452 may play an important role in LCFA-CoA binding and stabilization.

### **Binding of palmitoyl-CoA to the WT and mutant 89 residue L-CPTI peptides: displacement of bound *cis*-parinaroyl-CoA by palmitoyl-CoA**

Although the above studies demonstrated a high affinity of the WT L-CPTI for *cis*-parinaroyl-CoA, and that the tryptophan mutations dramatically decreased this affinity, it was important to determine if the C-terminal region of L-CPTI also bound endogenous ligands (e.g. palmitoyl-CoA) commonly oxidized by mitochondria of mammalian cells and tissues. To address this issue, the ability of palmitoyl-CoA to displace bound *cis*-parinaroyl-CoA from the 89 residue peptide was examined. Displacement of *cis*-parinaroyl-CoA from the WT L-CPTI peptide was very strong, resulting in approximately 70% displacement of *cis*-parinaroyl-CoA (Fig. 4b) and higher affinity for palmitoyl-CoA ( $K_i$  of  $2.7 \pm 0.5 \text{ nM}$ ) than *cis*-parinaroyl-CoA. However, palmitoyl-CoA binding of the mutant peptides resulted in only 50–60% *cis*-parinaroyl-CoA displacement and weaker affinity binding (Table 5) than the WT L-CPTI peptide—further confirming that the conserved C-terminal tryptophan residues are important in LCFA-CoA binding. Finally, the lower  $K_i$ s obtained for palmitoyl-CoA than the  $K_d$ s obtained for *cis*-parinaroyl-CoA indicated that L-CPTI and the mutant peptides had a somewhat stronger affinity for the endogenous ligand (palmitoyl-CoA) than *cis*-parinaroyl-CoA.

### **Direct binding of endogenous palmitoyl-CoA: quenching of L-CPTI 89 residue peptide intrinsic aromatic amino acid fluorescence**

To further establish the differential effects of the W391A and W452A mutations on ligand affinity and specificity of the peptide, advantage was taken of the intrinsic fluorescence properties of the L-CPTI C-terminal aromatic amino acids (two Trp and three Tyr residues). In this assay, quenching of the intrinsic aromatic amino acid fluorescence of the 89 residue peptides was examined in direct response to palmitoyl-CoA. With higher concentration of palmitoyl-CoA, the intrinsic aromatic amino acid fluorescence of the WT L-CPTI (Fig. 4c) and mutant peptides was increasingly quenched. Analysis of the quenching curves revealed high affinity binding ( $K_d = 4\text{--}16 \text{ nM}$ ), with each of the mutants having weaker affinities than the WT peptide. Thus, the results of the direct aromatic amino acid fluorescence quenching



by palmitoyl-CoA confirmed the data obtained with the *cis*-parinaroyl-CoA displacement assay (Table 5), and further suggested that the C-terminal peptide of L-CPTI and these conserved tryptophan residues are needed for high affinity LCFA-CoA binding. Furthermore, these data suggest that the decreased activity seen in the mutants is at least in part due to the decreased interaction of L-CPTI with ligand.

### **WT L-CPTI or mutant 89 residue peptide binding to *cis*-parinaroyl-CoA: fluorescence resonance energy transfer**

The above findings with intensity-based fluorescence assays were confirmed with an intermolecular distance-based fluorescence assay. The absorbance spectrum of *cis*-parinaroyl-CoA significantly overlaps the emission spectra of the aromatic amino acids in WT L-CPTI and mutant peptides upon excitation at 280nm—thereby allowing FRET and providing an independent means to confirm that WT L-CPTI and mutant peptides bound *cis*-parinaroyl-CoA with high affinity. FRET between the CPTI aromatic amino acid residues and bound *cis*-parinaroyl-CoA was measured from both the decrease in donor emission at 333nm and the appearance of sensitized acceptor (*cis*-parinaroyl-CoA) emission at 416nm (Fig. 5). With increasing concentration of *cis*-parinaroyl-CoA, the emission of WT L-CPTI was decreased concomitant with increased appearance of *cis*-parinaroyl-CoA sensitized emission (Fig. 5a). Examination of multiple titration curves allowed for determination of the binding affinity of CPTI for *cis*-parinaroyl-CoA under FRET conditions. Binding curves resolved a single *cis*-parinaroyl-CoA binding site with  $K_d$  of  $35 \pm 10$ nM calculated from quenching of WT CPTI amino acid fluorescence emission (Fig. 5b) and  $K_d$  of  $20 \pm 6$ nM determined from sensitized emission of bound *cis*-parinaroyl-CoA. These affinities were somewhat weaker than determined by the direct binding of *cis*-parinaroyl-CoA under non-FRET conditions (Fig. 4a)—likely due to greater sensitivity of the FRET assay to the relative orientation of CPTI aromatic amino acid residues with respect to the fluorescent LCFA-CoA within the binding site. Similar FRET assays also confirmed that W391A (Fig. 5c,d) and W452A (Fig. 5e,f) bound *cis*-parinaroyl-CoA with substantially weaker affinity than the WT (Table 6).

### **Close molecular proximity between aromatic amino acid residues in WT L-CPTI or mutant 89 residue peptides and bound *cis*-parinaroyl-CoA: fluorescence resonance energy transfer**

Since FRET is inversely proportional to the sixth-power of the distance between donor and acceptor, it is useful as a molecular distance ruler in the range of 1–100 Å depending on the specific donor-acceptor pair examined. FRET between the WT L-CPTI peptide and *cis*-parinaroyl-CoA yielded an intermolecular distance of  $28 \pm 1$ Å determined from the donor (L-CPTI) quenching and  $38 \pm 1$ Å determined from the increased acceptor (*cis*-parinaroyl-CoA) fluorescence (Fig. 5a). FRET between the mutant peptides and *cis*-parinaroyl-CoA yielded slightly closer intermolecular distances than for the WT (Table 6), suggesting that the conformational changes seen in Fig. 1 may play a role in decreasing the affinity for LCFA-CoA. Unfortunately, since FRET only provides the average energy transfer efficiency between all of the intrinsically fluorescent residues (5 for WT and 4 for each mutant), we cannot distinguish if some of these residues are now closer to the LCFA-CoA while other residues are further apart. However, the relative intermolecular distances were consistent with close molecular interaction rather than non-specific binding of the *cis*-parinaroyl-CoA by each of the examined L-CPTI peptides, and these data further confirm that the 89 residue C-terminal peptide is sufficient for interaction with LCFA-CoA.

## DISCUSSION

Carnitine palmitoyl transferase I is the rate limiting enzyme in mitochondrial oxidation of LCFAs. Although LCFA-CoAs themselves cannot enter the mitochondria, CPTI catalyzes the conversion of LCFA-CoA to LCFA-carnitine at the cytoplasmic face of the mitochondrial outer membrane. LCFA-carnitines are then transported into the mitochondria via additional proteins. Despite the importance of this key enzyme in energy homeostasis, an LCFA-CoA binding site has not yet been identified. Likewise, it is not clear whether cytoplasmic LCFA-CoA binding proteins directly interact with CPTI to regulate activity. The current investigation provides several new insights contributing to our understanding of these issues.

First, these data showed for the first time that the 89 residue C-terminal L-CPTI peptide was sufficient for strong molecular interaction/binding with cytoplasmic LCFA-CoA binding proteins. The C-terminal 89 residue L-CPTI peptide exhibited high affinity binding ( $K_d$ s of 2–8 nM) for cytoplasmic LCFA-CoA binding proteins in the order: L-FABP > ACBP > SCP-2. Interestingly, interaction of L-CPTI with the LCFA-CoA binding proteins decreased the proportion of  $\alpha$ -helix nearly 2-fold while concomitantly increasing other structures. While alanine mutation in Trp391 of L-CPTI did not alter affinity for cytoplasmic LCFA-CoA binding proteins, alanine substitution in the Trp452 residue reduced the affinity for cytoplasmic LCFA-CoA binding protein >10 fold.

Second, all the cytoplasmic LCFA-CoA binding proteins examined (L-FABP, ACBP, SCP-2) enhanced L-CPTI activity. These data suggested that: (i) the C-terminal 89-residue L-CPTI peptide was capable of converting LCFA-CoA to acyl-carnitine even in the absence of the integral membrane portion of the L-CPTI protein; (ii) the tryptophan residues at positions 391 and 452 were essential for activity of the C-terminal 89 residue L-CPTI; (iii) cytoplasmic LCFA-CoA binding proteins (ACBP, L-FABP, and SCP-2) were effective in enhancing L-CPTI activity; and (iv) L-FABP was the most efficient in enhancing L-CPTI activity of the proteins examined. Since previous studies with BSA have shown that mutation of W391A and W452A alters  $V_{max}$  but not the  $K_m$  for CPTI activity and since the data herein show similar results for the mutant peptides with each cytoplasmic LCFA-CoA binding protein [22], we predict that a similar effect is occurring in the presence of the cytoplasmic lipid binding proteins and that these mutations are affecting the stability of the enzyme substrate complex. Thus, the cytoplasmic LCFA-CoA binding proteins functioned at least as efficiently as BSA—indicating that cytoplasmic LCFA-CoA binding proteins can significantly contribute to L-CPTI activity.

Third, the L-CPTI C-terminal 89 residue peptide was identified as a high affinity LCFA-CoA binding domain. Due to lack of a 3D-structure for L-CPTI, the identity of the LCFA-CoA binding site had not previously been established. The current study presented evidence that endogenous palmitoyl-CoA directly binds to the L-CPTI C-terminal 89 residue peptide with very high affinity. In general, the fluorescence assays yielded a single high affinity binding site of the C-terminal 89 residue L-CPTI peptide for the naturally-occurring fluorescent (*cis*-parinaroyl-CoA) and non-fluorescent (palmitoyl-CoA) with  $K_d$  values of 3–35 nM—in the same range as the unbound LCFA-CoA concentration in the cytosol of living cells [11]. FRET between L-CPTI aromatic amino acid residues and bound *cis*-parinaroyl-CoA yielded an intermolecular distance of 25 Å—indicating close molecular interaction. These findings were consistent with naturally-occurring and endogenous LCFA-CoAs being physiologically significant ligands for CPTI. LCFA-CoA binding to the C-terminal 89 residue L-CPTI peptide significantly altered the peptide structure. Binding of palmitoyl-CoA significantly quenched the 89 residue peptide aromatic amino acid fluorescence emission, consistent with a reorientation of one or more of these residues from the more hydrophobic

interior of the protein to the more aqueous exposed protein surface. Similar conformational changes in response to ligand binding also occur in the cytoplasmic LCFA-CoA binding proteins ACBP, L-FABP, and SCP-2 [13, 14, 37].

The high affinities of the C-terminal 89 residue L-CPTI peptide for LCFA-CoAs were in the same range as those exhibited by cytoplasmic LCFA-CoA binding proteins such as ACBP, L-FABP, and SCP-2 measured with similar assays [13, 14, 37]. These data suggested that in the outer mitochondrial membrane, the cytoplasmic facing C-terminal domain of L-CPTI has sufficiently high LCFA-CoA affinity to compete effectively with cytoplasmic LCFA-CoA binding proteins such as ACBP, L-FABP, and SCP-2. This was supported by measurement of L-CPTI activity measured with increasing concentrations of these proteins and constant LCFA-CoA concentration. At low ratio of cytoplasmic LCFA-CoA binding protein/LCFA-CoA the activity of L-CPTI was enhanced, while at high ratios, the activity was less enhanced. Furthermore, since previous studies have reported that increasing concentrations of ACBP bound LCFA-CoA increase CPTI activity [6], the decreased activity seen with increasing ACBP and SCP-2 concentrations (constant LCFA-CoA concentration) suggest that LCFA-CoA may be substrate limiting, possibly due to the higher affinity of ACBP and SCP-2 for LCFA-CoA than L-FABP [6, 14, 34, 37]. The observation that the C-terminal 89 residue L-CPTI peptide exhibited high affinity for the palmitoyl-CoA may be taken in the context of the known structure of the ligand-binding pocket of the cytoplasmic LCFA-CoA binding protein ACBP. The predicted secondary structure of the 89 amino acid regions of L-CPTI containing these conserved residues consists of four  $\alpha$ -helices similar to the known 3-D structure of the ACBP with bound palmitoyl-CoA [38]—suggesting that this region of L-CPTI and M-CPTI spanning these conserved residues could be the palmitoyl-CoA binding site.

Although it is unlikely that these 89 amino acid peptides will fully mimic the structure of the full-length protein, significant differences were noted in their structures which could explain some of the differences in activity. For example, the increased proportion of  $\alpha$ -helices elicited by the W391A mutation resulted in decreased L-CPTI affinity for LCFA-CoA and activity but no effect on affinity for cytoplasmic LCFA-CoA binding proteins. In contrast, the decreased proportion of  $\alpha$ -helix induced by the W452A mutation resulted in a more severe phenotype, i.e. decreased LCFA-CoA binding activity, decreased affinity for cytoplasmic LCFA-CoA binding proteins, and decreased L-CPTI activity. Thus, the tryptophan residue at position 452, and less so that at 391, both significantly contribute not only to LCFA-CoA binding to L-CPTI, but also interaction of L-CPTI with cytoplasmic LCFA-CoA binding proteins—both contributing to L-CPTI activity. These findings suggest that the cytoplasmic LCFA-CoA binding proteins may regulate L-CPTI activity not only by binding/transporting LCFA-CoA in the cytoplasm, but also by directly interacting with the C-terminal L-CPTI domain to influence L-CPTI activity.

In summary, the data presented herein showed for the first time that the C-terminal 89 residue domain of L-CPTI was crucial in determining high affinity binding of cytoplasmic LCFA-CoA binding proteins, high affinity binding of LCFA-CoA, and CPTI activity. While the two tryptophan residues at positions 391 and 452 are not required for LCFA-CoA binding or cytoplasmic LCFA-CoA binding protein interaction, they significantly modify binding affinity and specificity. Some of these changes may be due to the tryptophan itself being important for binding and some of the changes may be due to the structural changes resulting from the amino acid substitution. These data demonstrated a direct interaction of the C terminal region of L-CPTI with cytoplasmic LCFA-CoA binding proteins which resulted in enhanced L-CPTI activity.

## Abbreviations

|                 |  |
|-----------------|--|
| <b>CPTI</b>     | carnitine palmitoyl transferase I                                |
| <b>L-CPTI</b>   | liver CPTI   |
| <b>WT</b>       | the C-terminal 89 amino acid cytoplasmic domain of L-CPTI        |
| <b>W391A</b>    | mutant of WT L-CPTI with alanine substitution for tryptophan 391 |
| <b>W452A</b>    | mutant of WT L-CPTI with alanine substitution for tryptophan 452 |
| <b>LCFA</b>     | long chain fatty acid  |
| <b>LCFA-CoA</b> | long chain fatty acyl CoA  |
| <b>ACBP</b>     | acyl CoA binding protein   |
| <b>L-FABP</b>   | liver fatty acid binding protein                                 |
| <b>SCP-2</b>    | sterol carrier protein-2   |

## Acknowledgments

This work was supported in part by the USPHS, National Institutes of Health grants DK77573 (H.A.H.), HL52571 and MRF Grant (G.W.), and DK41402 (F.S. and A.B.K.).

## REFERENCE LIST

1. McGarry JD. Travels with carnitine palmitoyltransferase I: from liver to germ cell with stops in between. *Biochem Soc Trans.* 2001; 29:241–245. [PubMed: 11356162]
2. Schroeder F, Huang H, Hostetler HA, et al. Stability of fatty acyl CoA thioester ligands of hepatocyte nuclear factor -4alpha and peroxisome proliferator-activated receptor alpha. *Lipids.* 2005; 40:559–568. [PubMed: 16149734]
3. Jolly CA, Chao H, Kier AB, Billheimer JT, Schroeder F. Sterol carrier protein-2 suppresses microsomal acyl CoA hydrolysis. *Mol Cell Biochem.* 2000; 205:83–90. [PubMed: 10821425]
4. Woldegiorgis G, Bremer J, Shrago E. Substrate inhibition of carnitine palmitoyltransferase by palmitoyl-CoA and activation by phospholipids and proteins. *Biochim Biophys Acta.* 1985; 837:135–140. [PubMed: 4052442]
5. Shi J, Zhu H, Arvidson DN, Woldegiorgis G. A single amino acid change (substitution of glutamate 3 with alanine) in the N-terminal region of rat liver carnitine palmitoyltransferase I abolishes malonyl-CoA inhibition and high affinity binding. *J Biol Chem.* 1999; 274:9421–9426. [PubMed: 10092622]
6. Abo-Hashema KAH, Cake MH, Lukas MA, Knudsen J. The interaction of acyl CoA with acyl CoA binding protein and carnitine palmitoyltransferase I. *Int J Biochem & Cell Biol.* 2001; 33:807–815. [PubMed: 11404184]
7. Prentki M, Corkey BE. Are the  $\beta$ -cell signaling molecules malonyl-Co-A and cytosolic long-chain Acyl-CoA implicated in multiple tissue defects of obesity and NIDDM? *Diabetes.* 1996; 45:273–283. [PubMed: 8593930]
8. Hirsch J. The search for new ways to treat obesity. *Proc Natl Acad Sci U S A.* 2002; 99:9096–9097. [PubMed: 12093927]
9. Bonnefont JP, Djouadi F, Prip-Buus C, et al. Carnitine palmitoyltransferase 1 and 2: biochemical, molecular and medical aspects. *Mol Aspects Med.* 2004; 25:495–520. [PubMed: 15363638]
10. Gossett RE, Frolov AA, Roths JB, et al. Acyl Co A binding proteins: multiplicity and function. *Lipids.* 1996; 31:895–918. [PubMed: 8882970]
11. Faergeman NJ, Knudsen J. Role of long-chain fatty acyl-CoA esters in the regulation of metabolism and in cell signalling. *Biochem J.* 1997; 323:1–12. [PubMed: 9173866]
12. McArthur MJ, Atshaves BP, Frolov A, et al. Cellular uptake and intracellular trafficking of long chain fatty acids. *J Lipid Res.* 1999; 40:1371–1383. [PubMed: 10428973]

13. Frolov A, Cho TH, Murphy EJ, Schroeder F. Isoforms of rat liver fatty acid binding protein differ in structure and affinity for fatty acids and fatty acyl CoAs. *Biochemistry*. 1997; 36:6545–6555. [PubMed: 9174372]
14. Frolov A, Cho TH, Billheimer JT, Schroeder F. Sterol carrier protein-2, a new fatty acyl coenzyme A-binding protein. *J Biol Chem*. 1996; 271:31878–31884. [PubMed: 8943231]
15. Gallegos AM, Atshaves BP, Storey SM, et al. Gene structure, intracellular localization, and functional roles of sterol carrier protein-2. *Prog Lipid Res*. 2001; 40:498–563. [PubMed: 11591437]
16. Rasmussen JT, Faergeman NJ, Kristiansen K, Knudsen J. Acyl-CoA-binding protein (ACBP) can mediate intermembrane acyl- CoA transport and donate acyl-CoA for beta-oxidation and glycerolipid synthesis. *Biochem J*. 1994; 299:165–170. [PubMed: 8166635]
17. Veerkamp JH, van Moerkerk HT. Fatty acid-binding protein and its relation to fatty acid oxidation. *Mol Cell Biochem*. 1993; 123:101–106. [PubMed: 8232250]
18. Atshaves BP, Storey SM, Schroeder F. Sterol carrier protein-2/sterol carrier protein-x expression differentially alters fatty acid metabolism in L-cell fibroblasts. *J Lipid Res*. 2003; 44:1751–1762. [PubMed: 12810824]
19. Atshaves BP, Storey S, Huang H, Schroeder F. Liver fatty acid binding protein expression enhances branched-chain fatty acid metabolism. *Mol Cell Biochem*. 2004; 259:115–129. [PubMed: 15124915]
20. Martin GG, Danneberg H, Kumar LS, et al. Decreased liver fatty acid binding capacity and altered liver lipid distribution in mice lacking the liver fatty acid binding protein (L-FABP) gene. *J Biol Chem*. 2003; 278:21429–21438. [PubMed: 12670956]
21. Seedorf U, Raabe M, Ellinghaus P, et al. Defective peroxisomal catabolism of branched fatty acyl coenzyme A in mice lacking the sterol carrier protein-2/sterol carrier protein-x gene function. *Genes and Development*. 1998; 12:1189–1201. [PubMed: 9553048]
22. Dai J, Zhu H, Shi J, Woldegiorgis G. Identification by mutagenesis of conserved arginine and tryptophan residues in rat liver carnitine palmitoyltransferase I important for catalytic activity. *J Biol Chem*. 2000; 275:22020–22024. [PubMed: 10801831]
23. Shi J, Zhu H, Arvidson DN, Woldegiorgis G. The first 28 N-terminal amino acid residues of human heart carnitine palmitoyltransferase I are essential for malonyl-CoA sensitivity and high affinity binding. *Biochem*. 2000; 39:712–717. [PubMed: 10651636]
24. Woldegiorgis G, Dai J, Arvidson DN. Structure-function studies with the mitochondrial carnitine palmitoyltransferases I and II. *Chemical Monthly (Austria)*. 2005; 136:1325–1340.
25. Shanmugasundaram T, Kumar GK, Wood HG. Involvement of tryptophan residues at the coenzyme A binding site of carbon monoxide dehydrogenase from *Clostridium thermoaceticum*. *Biochem*. 1988; 27:6499–6503. [PubMed: 3219350]
26. Chao H, Martin G, Russell WK, et al. Membrane charge and curvature determine interaction with acyl CoA binding protein (ACBP) and fatty acyl CoA targeting. *Biochemistry*. 2002; 41:10540–10553. [PubMed: 12173941]
27. Murphy EJ, Edmondson RD, Russell DH, Schroeder F. Isolation and characterization of two distinct forms of liver fatty acid binding protein from the rat. *Biochim Biophys Acta*. 1999; 1436:413–425. [PubMed: 9989272]
28. Hostetler HA, Petrescu AD, Kier AB, Schroeder F. Peroxisome proliferator activated receptor alpha (PPARalpha) interacts with high affinity and is conformationally responsive to endogenous ligands. *J Biol Chem*. 2005; 280:18667–18682. [PubMed: 15774422]
29. Hostetler HA, McIntosh AL, Atshaves BP, et al. Liver type Fatty Acid Binding Protein (L-FABP) interacts with peroxisome proliferator activated receptor- $\alpha$  in cultured primary hepatocytes. *J Lipid Res*. 2009; 50:1663–1675. [PubMed: 19289416]
30. Sreerama N, Woody R. Estimation of protein secondary structure from circular dichroism spectra; Comparison of CONTIN, SELCON, and DCSSTR methods with an expanded reference set. *Anal Biochem*. 2000; 287:252–260. [PubMed: 11112271]
31. Martin GG, Hostetler HA, McIntosh AL, et al. Structure and function of the sterol carrier protein-2 (SCP-2) N-terminal pre-sequence. *Biochem*. 2008; 47:5915–5934. [PubMed: 18465878]

32. Bremer J, Woldegiorgis G, Schalinske K, Shrago E. *Biochim Biophys Acta*. 1985; 833:9–16. [PubMed: 3967042]
33. Zhu H, Shi J, de Vries Y, et al. Functional studies of yeast-expressed human heart muscle carnitine palmitoyltransferase I. *Arch Biochem Biophys*. 1997; 347:53–61. [PubMed: 9344464]
34. Hubbell T, Behnke WD, Woodford JK, Schroeder F. Recombinant liver fatty acid binding protein interactions with fatty Acyl-Coenzyme A. *Biochemistry*. 1994; 33:3327–3334. [PubMed: 8136369]
35. Ellis J, Bagshaw CR, Shaw WV. Tryptophan fluorescence of chloramphenicol acetyltransferase: resolution of individual excited-state lifetimes by site-directed mutagenesis and multifrequency phase fluorometry. *Biochemistry*. 1995; 34:3513–3520. [PubMed: 7893646]
36. Wouters F, Bastiaens PI, Wirtz KW, Jovin TM. FRET microscopy demonstrates molecular association of non-specific lipid transfer protein (nsL-TP) with fatty acid oxidation enzymes. *EMBO J*. 1998; 17:7179–7189. [PubMed: 9857175]
37. Frolov AA, Schroeder F. Acyl coenzyme A binding protein: conformational sensitivity to long chain fatty acyl-CoA. *J Biol Chem*. 1998; 273:11049–11055. [PubMed: 9556588]
38. Kragelund BB, Knudsen J, Poulsen FM. Acyl-coenzyme A binding protein (ACBP). *Biochim Biophys Acta*. 1999; 1441:150–161. [PubMed: 10570243]

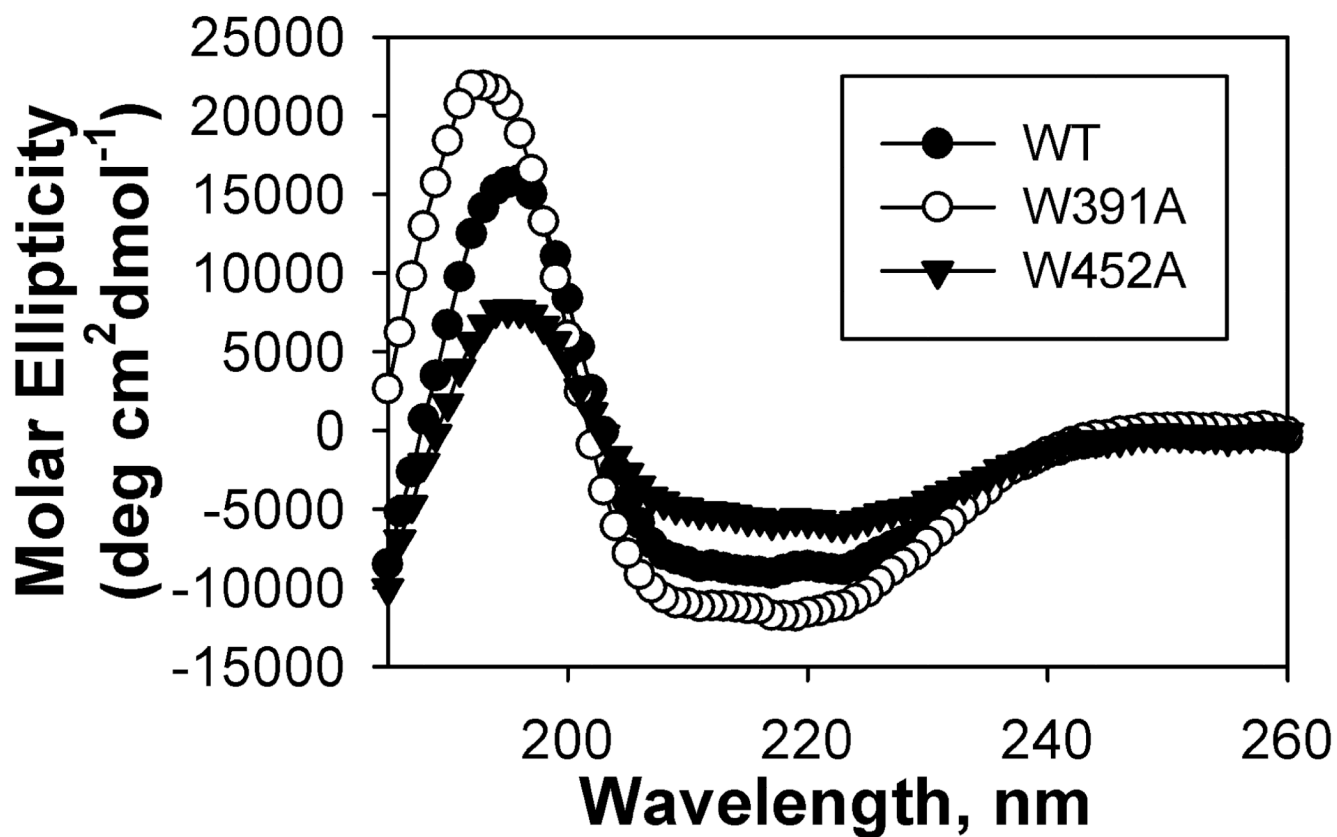


**Fig. 1. Circular dichroic spectra of L-CPTI mutant and wild type peptides**

Far ultraviolet (UV) circular dichroic (CD) spectra of 3.4 $\mu$ M CPTI C-terminal 89-residue (amino acids 381–469) wild type (WT, filled circles) or mutant (W391A, open circles; W452A, filled inverted triangles) peptides were obtained with a spectropolarimeter. Each spectrum represents an average of 10 scans for a given representative spectrum from three replicates.

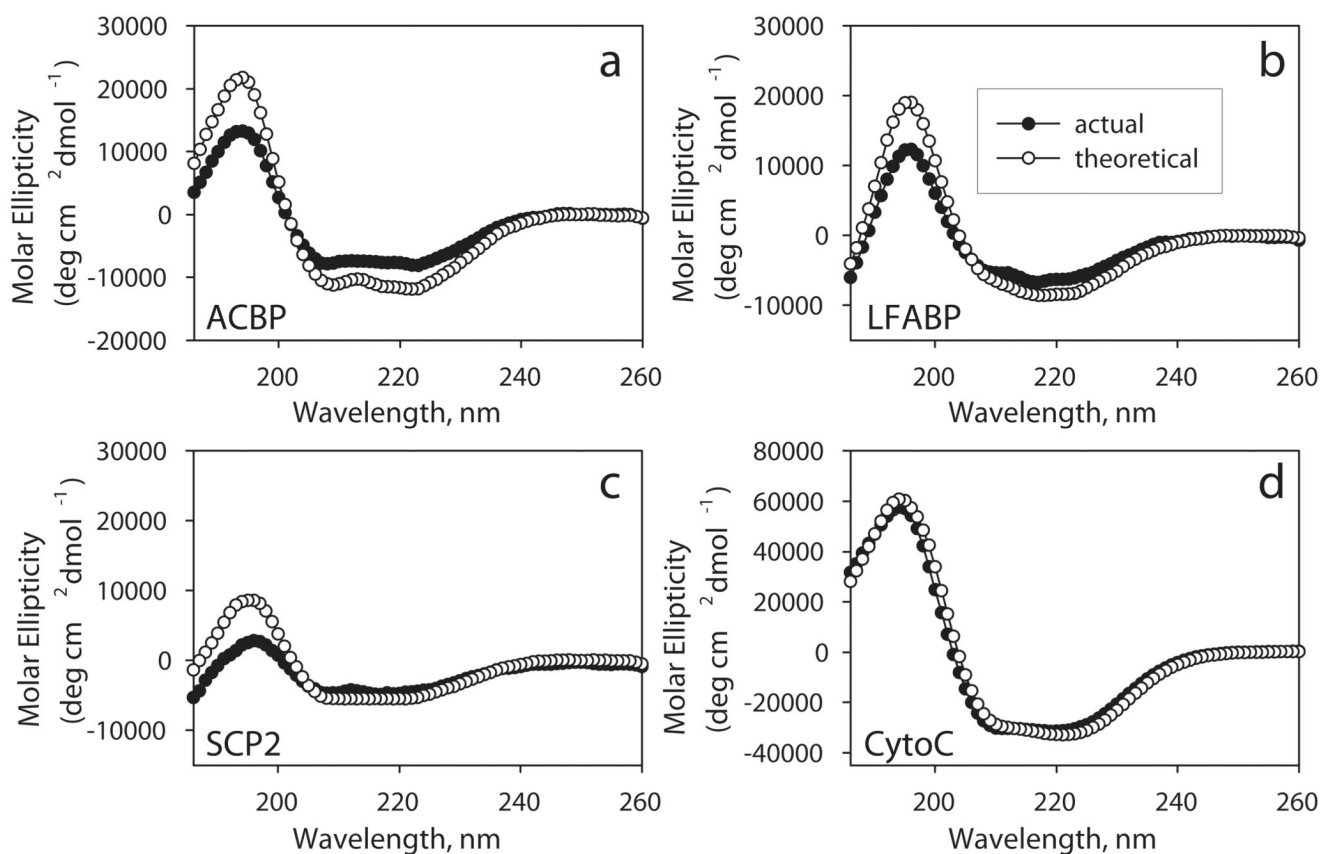


**Fig. 2. CD of WT CPTI peptide with ACBP, L-FABP, and SCP-2**

(a) Far-UV circular dichroic (CD) spectra of a mixture of equal amino acid molarities of the WT L-CPTI peptide with ACBP (*filled circles*) as compared to the theoretically expected spectrum (*open circles*). The theoretically expected value of the combined proteins assuming no interaction was determined by averaging the spectra of each protein analyzed separately at a concentration equal to that in the mixture. Comparison of the far-UV CD spectra of WT L-CPT peptide and L-FABP (b), SCP-2 (c), or cytochrome C (d) obtained experimentally (*filled circles*) and the theoretically expected spectrum (*open circles*). Each spectrum represents an average of 10 scans for a given representative spectrum from three replicates.



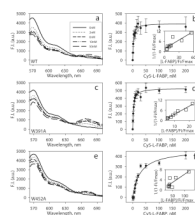


**Fig. 3. FRET from Cy3-labeled CPTI peptides to Cy5-labeled L-FABP**

Recombinant WT L-CPTI C-terminal 89-residue peptide and LCFA-CoA binding proteins were chemically labeled with fluorescent Cy3 and Cy5 dyes, respectively as described in “Experimental procedures” section. All spectra were corrected for background fluorescence. Emission spectra of Cy3-WT CPTI (a), Cy3-W391A (c), or Cy3-W452A (e) peptide and Cy5-L-FABP upon excitation at 550nm at 0, 2, 6, 10 and 50nM Cy5-L-FABP. FRET from donor Cy3-CPTI to acceptor Cy5-L-FABP was detected as quenching of Cy3 fluorescence emission (near 570nm) and as the appearance of sensitized Cy5 emission (near 675nm). (B) By plotting the change in maximal fluorescence intensity at ~675nm due to the sensitized emission of Cy5 fluorescence as a function of Cy5-L-FABP concentration, saturable binding curves were obtained for WT CPTI (b), W391A (d), and W452A (f) which allowed for the calculation of the protein binding affinity. *Inset* referring to a linear plot of the binding curve. Values represent the mean  $\pm$  SE, n = 4.

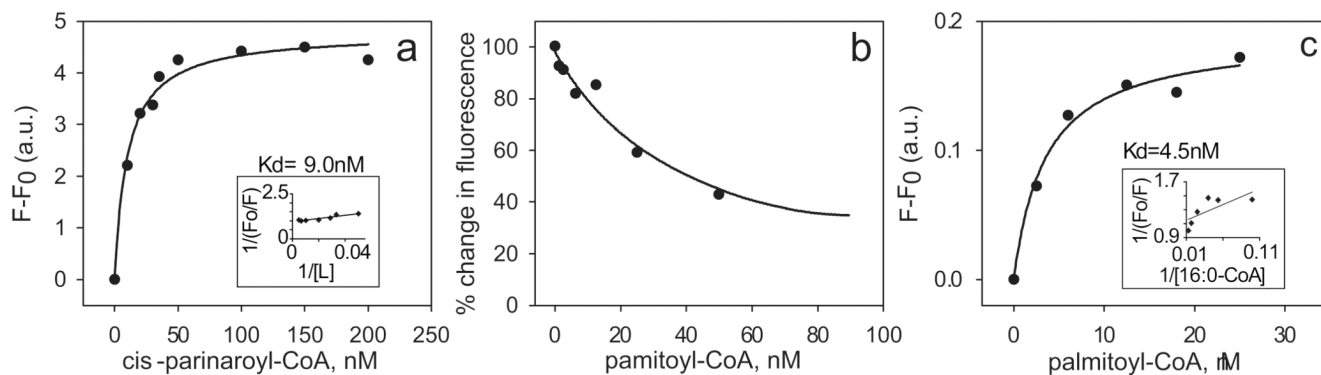


**Fig. 4. Fluorescent ligand binding assays of L-CPTI C-terminal WT peptide with LCFA-CoA**  
**(a)** Direct binding of the fluorescent LCFA derivative, *cis*-parinaroyl-CoA, by the WT CPTI C-terminal peptide. The maximal fluorescence emission for *cis*-parinaroyl-CoA (measured at 416nm upon excitation at 312nm) in the presence of 0.1 $\mu$ M WT CPTI 89 residue peptide was plotted as a function of increasing *cis*-parinaroyl-CoA concentration. *Inset*, Linear plot of the binding curve data for number of binding sites. **(b)** Displacement of CPTI-bound *cis*-parinaroyl-CoA by palmitoyl-CoA. For the displacement of peptide bound *cis*-parinaroyl-CoA by palmitoyl-CoA, 0.1 $\mu$ M of the 89 residue WT peptide was incubated with 50nM *cis*-parinaroyl-CoA for 5 min at 24 $^{\circ}$ C to obtain maximal fluorescence. This mixture was titrated with palmitoyl-CoA (0–150nM), and fluorescence intensities were measured at 426nm upon excitation of *cis*-parinaroyl-CoA at 310 nm. The percent change in fluorescence intensity was plotted as a function of palmitoyl-CoA concentration. **(c)** Direct binding of palmitoyl-CoA determined by quenching of CPTI aromatic amino acid fluorescence. For quenching of aromatic amino acid fluorescence, the WT CPTI peptide was titrated with increasing concentrations of palmitoyl-CoA, and emission at 333nm was measured upon excitation at 280nm. Data are presented as the change in fluorescence intensity (F<sub>0</sub>-F) at each titration point (i.e. concentration of palmitoyl-CoA). The *inset* shows the linear plot of the ligand binding data. All fluorescence emission spectra were corrected for background signal of ligand alone in buffer and CPTI peptide alone in buffer as described in “Experimental procedures” section. All plots are the mean values from 5 replicates.

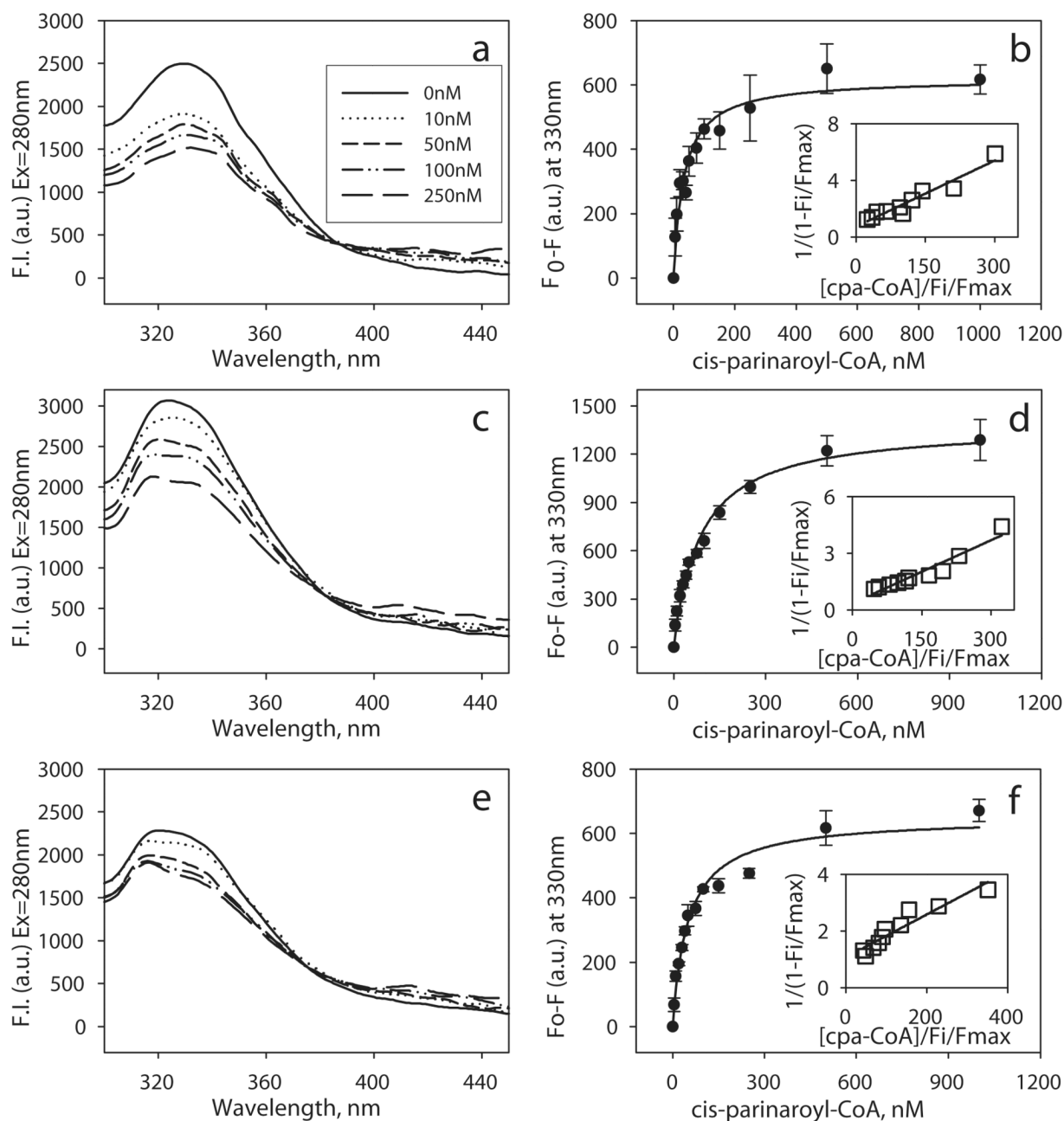


**Fig. 5. Fluorescence resonance energy transfer (FRET) from CPTI aromatic amino acids to bound *cis*-parinaroyl-CoA: intermolecular distance and FRET binding assay**

FRET from CPTI peptide (0.1 $\mu$ M) aromatic amino acids to bound *cis*-parinaroyl-CoA acid was measured by excitation at 280nm in the presence of increasing *cis*-parinaroyl-CoA (0–250nM) concentration and corrected for background fluorescence. FRET was detected as quenching of CPTI aromatic amino acid fluorescence emission near 330nm and as appearance of sensitized emission from CPTI bound *cis*-parinaroyl-CoA near 420nm for the WT (a) W391A (c), and W452A (e) mutant peptides. Each spectrum is of the average from 5 replicates. A saturable binding curve was obtained by plotting the change in maximal

fluorescence intensity at 330nm as a function of cis-parinaroyl-CoA concentration for WT **(b)**, W391A **(d)**, and W452A **(f)**. Binding curve values represent the mean  $\pm$  SE, n=5.

**Table 1**  
**Percent composition of CPTI peptide secondary structure determined by circular dichroism**

The relative proportions of the different types of secondary structure for the CPTI mutant and wild type peptides were calculated as described in “Materials and Methods”. These structures were as follows: H(r) represents regular  $\alpha$ -helices, H(d) represents distorted  $\alpha$ -helices, S(r) represents regular  $\beta$ -sheets, S(d) represents distorted  $\beta$ -sheets, Turns represent  $\beta$ -turns, and Unrd represents unordered structures.

| CPTI  | Hr (%)  | Hd (%)     | Sr (%)     | Sd (%)      | Turns (%) | Unrd (%) |
|-------|---------|------------|------------|-------------|-----------|----------|
| WT    | 16±1    | 13±1       | 15.7±0.8   | 10.7±0.4    | 22.6±0.6  | 23±1     |
| W391A | 20±1 *  | 16.1±0.9 * | 8.4±0.4 ** | 8.5±0.3 *   | 23.0±0.6  | 24±1     |
| W452A | 6±1 **# | 8±1 **     | 18±1 #     | 12.3±0.4 ** | 24±1      | 29±1 **  |

Asterisks represent significant differences from wild type; (\* P<0.05, \*\* P<0.0001).

Pound signs represent significant differences between W452A and W391A (# P<0.05).

**Table 2**  
**Percent composition of WT CPT-I bound to ACBP, L-FABP, and SCP-2 secondary structures determined by CD**

The relative proportions of the different types of secondary structures for the wild type CPTI peptide were calculated as described in "Materials and Methods". These structures were as follows: H(r) represents regular  $\alpha$ -helices, H(d) represents distorted  $\alpha$ -helices, S(r) represents regular  $\beta$ -sheets, S(d) represents distorted  $\beta$ -sheets, Turns represent  $\beta$ -turns, and Unrd represents unordered structures.

| CoA BP | Spectra | Hr (%)       | Hd (%)       | Sr (%)       | Sd (%)       | Turns (%)  | Unrd (%)     |
|--------|---------|--------------|--------------|--------------|--------------|------------|--------------|
| ACBP   | Act     | 13.2±0.6**** | 13.1±0.1**** | 13.8±0.4**** | 9.5±0.1****  | 22.0±0.2   | 28.2±0.5***  |
|        | Theor   | 22.0±0.4     | 17.1±0.3     | 6.3±0.6      | 6.7±0.2      | 22.6±0.4   | 25.4±0.8     |
| L-FABP | Act     | 7.5±0.5***   | 9.1±0.4**    | 19.6±0.7**** | 12.2±0.2**** | 24.2±0.2** | 28.1±0.5     |
|        | Theor   | 14±1         | 11.7±0.7     | 16.1±0.2     | 10.7±0.3     | 22.1±0.6   | 26±1         |
| SCP-2  | Act     | 2.7±0.4***   | 5.5±0.3****  | 20.9±0.3     | 12.1±0.1**   | 24.2±0.5*  | 34.4±0.9**** |
|        | Theor   | 6.1±0.4      | 8.7±0.7      | 21.5±0.8     | 11.5±0.1     | 22.2±0.5   | 27.8±0.5     |
| CytoC  | Act     | 43±3         | 24±3         | 4±2          | 5±3          | 13.7±0.8   | 14±2         |
|        | Theor   | 46±2         | 25±4         | 4.4±0.7      | 5±1          | 11.4±0.7   | 11±4         |

Asterisks represent significant differences between experimentally acquired data (Act) versus the theoretical average of the proteins assuming no conformational change (Theor) with \* P<0.05, \*\* P<0.001, \*\*\* P<0.0001.

**Table 3**  
**Binding affinity and intermolecular distance between Cy3-labeled CPTI peptides and Cy5-labeled LCFA-CoA binding proteins: FRET results**

Values were calculated based upon the sensitized emission of acceptor (Cy5) fluorescence as a function of increasing acceptor concentration. Values represent the mean value  $\pm$  the standard error, n = 4. N.D. stands for not detected.

| FRET pair |          | Sensitized Emission |                    |
|-----------|----------|---------------------|--------------------|
| Donor     | Acceptor | $K_d$ (nM)          | R ( $\text{\AA}$ ) |
| CPTI WT   | ACBP     | $5 \pm 1$           | $56 \pm 1$         |
|           | L-FABP   | $2.5 \pm 0.8$       | $56 \pm 3$         |
|           | SCP-2    | $8 \pm 2$           | $61.5 \pm 0.9$     |
|           | CytoC    | N.D.                | N.D.               |
| W391A     | ACBP     | $6 \pm 1$           | $65 \pm 1$         |
|           | L-FABP   | $3.0 \pm 0.6$       | $50 \pm 2$         |
|           | SCP-2    | $7 \pm 1$           | $49 \pm 2$         |
|           | CytoC    | N.D.                | N.D.               |
| W452A     | ACBP     | $53 \pm 9$          | $65.8 \pm 0.2$     |
|           | L-FABP   | $28 \pm 5$          | $82 \pm 1$         |
|           | SCP-2    | $30 \pm 10$         | $68 \pm 2$         |
|           | CytoC    | N.D.                | N.D.               |

**Table 4**  
**CPTI activity with BSA, ACBP, L-FABP, or SCP-2 as the LCFA-CoA donor**

Mitochondria were isolated from the yeast strains separately expressing the wild-type and mutant CPTIs and then assayed for CPTI activity (as described in the Materials and Methods section) in the presence of 15, 30, 60 $\mu$ M, respectively of each of the LCFA-CoA donor proteins at a molar ratio of palmitoyl-CoA to protein of 7.41, 3.70, and 1.85. Values represent the means  $\pm$  standard deviation, n=5.

| Protein | Concentration | WT   | W391A         | W452A         |
|---------|---------------|--|---------------|---------------|
|         |               | <i>nmol•min<sup>-1</sup>•mg<sup>-1</sup></i> |               |               |
| BSA     | 15 $\mu$ M    | 33.7 $\pm$ 2.8                               | 6.6 $\pm$ 0.2 | 1.3 $\pm$ 0.3 |
|         | 30 $\mu$ M    | 24.3 $\pm$ 0.4                               | 7.0 $\pm$ 0.1 | 1.6 $\pm$ 0.2 |
|         | 60 $\mu$ M    | 15.9 $\pm$ 0.3                               | 4.4 $\pm$ 0.3 | 1.2 $\pm$ 0.2 |
| ACBP    | 15 $\mu$ M    | 31.8 $\pm$ 2.1                               | 3.3 $\pm$ 0.1 | 0.7 $\pm$ 0.2 |
|         | 30 $\mu$ M    | 27.6 $\pm$ 2.4                               | 4.5 $\pm$ 0.9 | 0.8 $\pm$ 0.2 |
|         | 60 $\mu$ M    | 13.2 $\pm$ 0.1                               | 5.7 $\pm$ 0.1 | 1.3 $\pm$ 0.1 |
| L-FABP  | 15 $\mu$ M    | 39.3 $\pm$ 2.5                               | 4.2 $\pm$ 0.1 | 0.9 $\pm$ 0.2 |
|         | 30 $\mu$ M    | 37.6 $\pm$ 0.1                               | 5.9 $\pm$ 0.1 | 1.1 $\pm$ 0.1 |
|         | 60 $\mu$ M    | 34.0 $\pm$ 0.1                               | 7.4 $\pm$ 0.1 | 1.6 $\pm$ 0.1 |
| SCP-2   | 15 $\mu$ M    | 31.7 $\pm$ 1.1                               | 4.7 $\pm$ 0.1 | 0.8 $\pm$ 0.2 |
|         | 30 $\mu$ M    | 26.1 $\pm$ 1.1                               | 5.7 $\pm$ 0.2 | 1.2 $\pm$ 0.2 |
|         | 60 $\mu$ M    | 16.5 $\pm$ 0.1                               | 4.5 $\pm$ 0.1 | 0.9 $\pm$ 0.2 |



**Table 5**  
**Binding affinity of CPTI peptides for *cis*-parinaroyl-CoA and palmitoyl-CoA**

Values represent the mean value  $\pm$  the standard error, n = 5.

|         | Cpn-CoA<br>$K_d$ (nM) | Displacement<br>$K_I$ (nM) | Quenching<br>$K_d$ (nM) |
|---------|-----------------------|----------------------------|-------------------------|
| CPTI WT | 9 $\pm$ 1             | 2.7 $\pm$ 0.5              | 5 $\pm$ 1               |
| W391A   | 52 $\pm$ 8            | 7 $\pm$ 1                  | 9 $\pm$ 1               |
| W452A   | 67 $\pm$ 10           | 17 $\pm$ 3                 | 16 $\pm$ 2              |

**Table 6**  
**Binding affinity and intermolecular distance between CPTI peptides and *cis*-parinaroyl-CoA: FRET results**

Values were calculated based upon the decrease in donor fluorescence (CPTI) as a function of increasing acceptor concentration. Values represent the mean value  $\pm$  the standard error,  $n = 5$ .

| Donor   | Donor Emission |                    |
|---------|----------------|--------------------|
|         | $K_d$ (nM)     | R ( $\text{\AA}$ ) |
| CPTI WT | $35 \pm 10$    | $28 \pm 1$         |
| W391A   | $88 \pm 9$     | $23.9 \pm 0.6$     |
| W452A   | $51 \pm 5$     | $24.3 \pm 0.6$     |